ELSEVIER

FEMS Microbiology Ecology 49 (2004) 319–332

FEMS MICROBIOLOGY Ecology

www.fems-microbiology.org

Detection of forest stand-level spatial structure in ectomycorrhizal fungal communities

Erik A. Lilleskov [a,*], Thomas D. Bruns [b], Thomas R. Horton [c], D. Lee Taylor [d], Paul Grogan [e]

[a] *USDA Forest Service, North Central Research Station, Forestry Sciences Laboratory, 410 MacInnes Dr., Houghton, MI 49931, USA*
[b] *Department of Plant and Microbial Biology, 111 Koshland Hall, University of California, Berkeley, CA 94720, USA*
[c] *SUNY-College of Environmental Science and Forestry, Faculty of Environmental and Forest Biology, 350 Illick Hall Syracuse, NY 13210, USA*
[d] *Institute of Arctic Biology, P.O. Box 757000, University of Alaska, Fairbanks AK 99775, USA*
[e] *Department of Biology, Queen's University, Kingston, Ont., Canada K7L 3N6*

Received 8 October 2003; received in revised form 2 April 2004; accepted 2 April 2004

First published online 10 May 2004

Abstract

Ectomycorrhizal fungal (EMF) communities are highly diverse at the stand level. To begin to understand what might lead to such diversity, and to improve sampling designs, we investigated the spatial structure of these communities. We used EMF community data from a number of studies carried out in seven mature and one recently fire-initiated forest stand. We applied various measures of spatial pattern to characterize distributions at EMF community and species levels: Mantel tests, Mantel correlograms, variance/mean and standardized variograms. Mantel tests indicated that in four of eight sites community similarity decreased with distance, whereas Mantel correlograms also found spatial autocorrelation in those four plus two additional sites. In all but one of these sites elevated similarity was evident only at relatively small spatial scales ($<$2.6 m), whereas one exhibited a larger scale pattern ($\sim$25 m). Evenness of biomass distribution among cores varied widely among taxa. Standardized variograms indicated that most of the dominant taxa showed patchiness at a scale of less than 3 m, with a range from 0 to $\geqslant$17 m. These results have implications for both sampling scale and intensity to achieve maximum efficiency of community sampling. In the systems we examined, cores should be at least 3 m apart to achieve the greatest sampling efficiency for stand-level community analysis. In some cases even this spacing may result in reduced sampling efficiency arising from patterns of spatial autocorrelation. Interpretation of the causes and significance of these patterns requires information on the genetic identity of individuals in the communities.

Keywords: Ectomycorrhizal fungi; Spatial autocorrelation; Spatial structure; Community structure; Mantel test; Mantel correlogram; Standardized variogram

1. Introduction

Ectomycorrhizal fungal (EMF) communities are quite diverse. Molecular analyses have revealed that in small monospecific forest stands there can be over 50 EMF species [1]. It is essential that we learn more about the spatial structure of these communities, both to constrain the universe of explanatory models for this local diversity [2], and to sample these communities effectively [3].

Relatively little is known about how EMF communities are structured spatially [3]. It is important to know whether communities as a whole, and individual species, exhibit distinctive spatial patterns, as a basis

* Corresponding author. Tel.: +1-906-482-6303x18; fax: +1-906-482-6355/4995.
E-mail address: elilleskov@fs.fed.us (E.A. Lilleskov).

0168-6496/$22.00
doi:10.1016/j.femsec.2004.04.004

for future investigation into the ecological processes generating such spatial patterns. A variety of processes could lead to species-specific spatial patterns in EMF populations, including variation in rates of genet growth (if patches are made up of one individual), internal structure of genets, or patterns of intraspecific establishment or survival that lead to clusters of individuals. These could be either endogenous (e.g., dimon mating, variable inoculum inputs) or exogenous (e.g., variation in resource availability or disturbance intensity that affect the patterns of EMF root colonization and survival). From our knowledge of differences among taxa in extramatrical hyphal anatomy (e.g., presence or absence of rhizomorphs, formation of hyphal mats [4]) we expect that taxa would be likely to differ in spatial colonization patterns, with species likely to differ in internal genet structure and rates of vegetative expansion. Sporocarp-based studies of EMF genet size have found that genets may vary from tens of centimeters, e.g., in some *Russula* species [5]; to tens of meters, e.g., in *Suillus* and *Boletus* (*Xerocomus*) spp. [6–10]. Even though some genets are large, they may exhibit internal spatial structure at smaller scales, because expanding genets might exhibit internal fragmentation [11] or more intense colonization of microsites. Furthermore, species may exhibit different genet-size patterns at different sites [10,11]. At the community level, processes that could lead to structuring include positive or negative species interactions, or convergent or divergent resource requirements or responses to disturbance [2,12].

We also wished to determine whether spatial analysis could help in determination of appropriate spatial scales for sampling EMF communities. Previous authors have indicated the need for more explicit information on spatial structure in ectomycorrhizal fungal communities in order to design more effective sampling strategies [1,3]. In particular, knowing the scales of spatial autocorrelation (i.e., patchiness) in EMF community structure can ensure that sampling is carried out at scales that are larger than these patches, thus leading to more information gained about the community composition and structure per sample.

Previous investigations of EMF community spatial pattern range from descriptive, e.g., [8,13] to statistical [14,15]. One study used Mantel tests [16] to analyze spatial structure of EMF communities [17] (for an application of geostatistical methods to arbuscular mycorrhizal spores, see [18]). We applied similar methods to a group of datasets from a range of forest types, with resolution at smaller spatial scales than in previous community studies, by combining molecular identification methods with abundance data from individual cores. Our approach was to investigate community-level spatial patterns using Mantel tests and Mantel correlograms, and to apply geostatistical and other methods to the species-level patterns of abundance.

2. Methods

2.1. Dataset description

The datasets were derived from a number of studies of ectomycorrhizal communities in California and the Pacific Northwest (Table 1). Stand age, canopy composition, and sampling scale varied among studies (Table 1). All studies used molecular genetic methods to identify EMF, and were carried out in mature forests using similar methods of soil coring, except for one, that examined a seral shrub community and associated Douglas-fir seedlings [19]; and another assayed species composition on the root system of excavated seedlings [15]. The molecular genetic methods used typically identified fungi on roots to the species or higher taxonomic level. Individuals within populations could not be distinguished by these methods, so it is impossible to determine whether repeat occurrences of a taxon in different cores represent the same or different individuals.

2.2. Spatial pattern analysis

The analysis of pattern was carried out at both the community and the species level. Each core or seedling was treated as the sampling unit. The community was described within the sampling unit using biomass of the root tips occupied by a species as our measure of abundance.

2.2.1. Community level analysis

Mantel tests [16] were used to determine whether spatial distance could explain a significant proportion of the variation in community composition among cores (i.e., if cores that were closer to each other were more or less similar than cores that were farther apart). Mantel tests allow comparison of the linear relationship among matrices where dependence among sampling points is likely. This dependence precludes standard regression approaches, which assume independence. We used the Mantel test protocol in the PC-ORD, Version 4 software [20]. We ran the Mantel tests of community dissimilarity (calculated as relative Sorensen dissimilarity) vs. a Euclidian distance matrix [20]. To calculate significance, the data were subjected to Monte Carlo randomization tests (1000 runs). The Mantel test outputs of pair-wise distances were then plotted, and fitted with an exponential rise to the maximum (single, three parameter), and a Loess smoothing fit in Sigmaplot 2002 for Windows Version 8.0. The equation for the exponential rise to the max-

Table 1
Summary of selected study site characteristics and sampling methods for the different studies included in the analysis

Study site	Lat./Long.	Dominant tree species	Stand age or tree dbh	Core diam. × depth (cm)	No. of cores or seedlings	Sampling range (m)[a]	Sampling design	Ref.
Sierra National Forest (SNF)	36°58′48″N/ 119°8′13″W	*Pinus ponderosa*[b]	Mature, 27–87 cm dbh	4 × 40	42	0.25–300	6 unevenly-spaced 1 × 1 m plots, cores in regular grid	[36]
HJ Andrews Experimental Forest (HJA)	44°15′30″N, 122°10′36″W	*Pseudotsuga menziesii*, *Tsuga heterophylla*	300 yrs	5 × 30	24	2[c]–49	50 m transect, cores evenly spaced at 2 m intervals	Horton, unpub.
Point Reyes National Seashore (PR BP seedling)	38°03′9″N, 122°50′24″W	*Pinus muricata*	Seedlings, <1 yr	NA[d]	39	0.07–45	7 random plot pairs (0.25 × 0.25m), 3 seedlings/plot	[15]
Point Reyes National Seashore (PR BPDF)	38°2′58″N, 122°51′1″W	*P. muricata*, *P. menziesii*	35 yrs	10 × 40	25	0.57–30	5 unevenly-spaced, 2–3 m transects, cores evenly spaced on transects	[37]
Marin County, CA (Manz)	37°54′96″N, 122°36′83″W	*P. menziesii* *Arctostaphylos glandulosa*	Seedlings (*P.m.*), mature (*A.g.*)	10 × 40	12	5–29	3 transects, ~10 m apart, 5 m spacing on transects	[19]
Point Reyes National Seashore (PR BP)	38°04′10″N, 122°50′24″W	*P. muricata*	34–38 yrs	10 × 40	15	1–22	5 plots, 3 cores/plot 1 m apart, 5–7 m between plots, rough transect	[13]
Salt Point State Park (SP2)	38°34′31″N, 123°18′43″W	*P. muricata*	~40 yrs	4 × 35	27	0.42–6.2	9 1 × 1.2 m evenly-spaced plots, 3 cores per plot in stratified random pattern	Lilleskov and Bruns, unpub.
Salt Point State Park (SP1)	38°34′31″N, 123°18′43″W	*P. muricata*	~40 yrs	10 × 35	27	0.42–6.2	9 1 × 1.2 m evenly-spaced plots, 3 cores per plot in stratified random pattern	Lilleskov and Bruns, unpub.

Studies are listed by sampling scale, in descending order.
[a] Minimum and maximum distance between cores or seedlings.
[b] *P. ponderosa* trees were sampled in the presence of a few sub-arboreal *Quercus*.
[c] One pair of cores were 1 m apart, all others were 2 m apart.
[d] Not applicable, seedlings excavated from soil.

imum was used to estimate the distance (in m) at which 95% and 99% of the background Sørensen's community dissimilarity was encountered.

As another estimate of the spatial scale at which communities were spatially autocorrelated, we performed mantel correlograms in the R Package [21]. Mantel correlograms are a multivariate method for examining scales of spatial autocorrelation, similar to the univariate methods described below. One advantage they have over regular Mantel tests is that nonlinear patterns are more likely to be revealed, because the linear comparisons are made between multiple shorter distance classes and the entire dataset, rather than for the whole dataset. As for the regular Mantel test, indices of community similarity are calculated for pairs of cores. We used two indices of similarity (in contrast to dissimilarity indices used for the Mantel tests above). Neither index uses double zeros to calculate similarity. The first is binary (Sørensen's coefficient) and the second is quantitative (Steinhaus coefficient) [21]. The pair-wise similarities were then divided into distance classes, and Mantel tests were calculated on each distance class, using a permutation method with 999 iterations to determine significance, with Bonferroni correction based on the number of distance classes tested, $\alpha = 0.05$. Positive, significant results in the smaller distance classes indicate positive spatial autocorrelation.

2.2.2. Individual taxon level analysis

To examine whether individual taxa differed in their distribution among cores, we used two approaches. First, we examined distribution of biomass among cores using frequency, relative abundance, frequency/relative abundance and variance/mean for individual taxa. We define relative abundance as the percentage of total EMF root tip biomass at a site represented by a species, and frequency as the percentage of cores or seedlings occupied by a species. High relative abundance and low frequency indicate biomass clumping, whereas low abundance and high frequency indicate dispersion of biomass among cores. Similarly, the variance to mean ratio is a metric of how evenly biomass is distributed among cores [22]. The lower the ratio, the more evenly biomass is distributed among cores. In analysis of distribution of individuals, the random distribution is assumed to be a Poisson distribution. For the Poisson distribution, the expectation is that the variance to mean ratio will be 1. Deviations above 1 indicate clumping, below 1 indicate dispersion. In the present case, we are looking at the variance to mean ratio of relative biomass rather than individuals, so the expectation of 1 for a variance/mean might not be strictly appropriate. Instead we will use it as a relative metric of differences among taxa.

We tested whether relative abundance, relative frequency, and variance/mean varied among taxonomic groups. To do this, we examined only species occurrences with high relative biomass (>10%) or relative frequency (>15%) at a site. Species with both low biomass and low frequency were excluded, because these taxa were uninformative about biomass distribution among cores. Across studies we combined species into higher taxonomic groups to enable comparisons (see Appendix A); this assumes that related species will exhibit similar spatial patterns, an assumption we will revisit in the discussion. Variance/mean data were $\log_{10}$ transformed to achieve normality. We subjected these data to either regular ANOVA (relative frequency and variance/mean), or Welch ANOVA in cases where tests indicated variances were unequal (relative biomass, relative biomass/relative frequency), using the JMP Version 3 software package [23]. Five taxonomic groups occurred sufficiently frequently (i.e., occurring in multiple studies, and in some cases multiple species within a study) for analysis: *Cenococcum geophilum* ($n = 6$), Thelephoroid (*Thelephora, Tomentella*, and other Thelephoraceae spp.) ($n = 8$), Russuloid (*Russula, Lactarius, Martellia*, and other Russulaceae spp.) ($n = 17$), Suilloid (*Suillus* and *Rhizopogon* spp.) ($n = 6$), Corticioid (*Amphinema byssoides, Piloderma, Byssocorticium*-like and other Corticiaceae spp.) ($n = 5$). To minimize stand age effects, we excluded all species from the seedling study, focusing only on species from mature stands. We also excluded groups with a low number of species or poor representation across sites (Boletoid, *Amanita*, and other ascomycetes all had two species occurrences; Cortinariaceae had three species occurrences, but all from the same site).

All of the above metrics are zero-dimensional, i.e., they do not take into account the spatial relationship among cores. In order to determine whether the patterns were dependent on the spatial scale of the sample, for taxa that occurred in multiple plots, we performed regressions of relative frequency, relative biomass and variance/mean vs. the farthest distance between cores at a site.

We also examined the scale at which species were clumped using standardized variograms, with the geostatistical program Variowin 2.2 [24]. This method reveals patterns of variance among cores over a range of distances. We chose standardized variograms, which correct for variance among cores at the endpoints during the calculation of variance between cores separated by a specified distance, because they were more robust in tests of artificial datasets when compared with nonstandardized variograms [25]. We fitted a spherical model to all data, except for a few species for which a Gaussian model gave a much better fit. For this analysis we focused again on the dominant taxa.

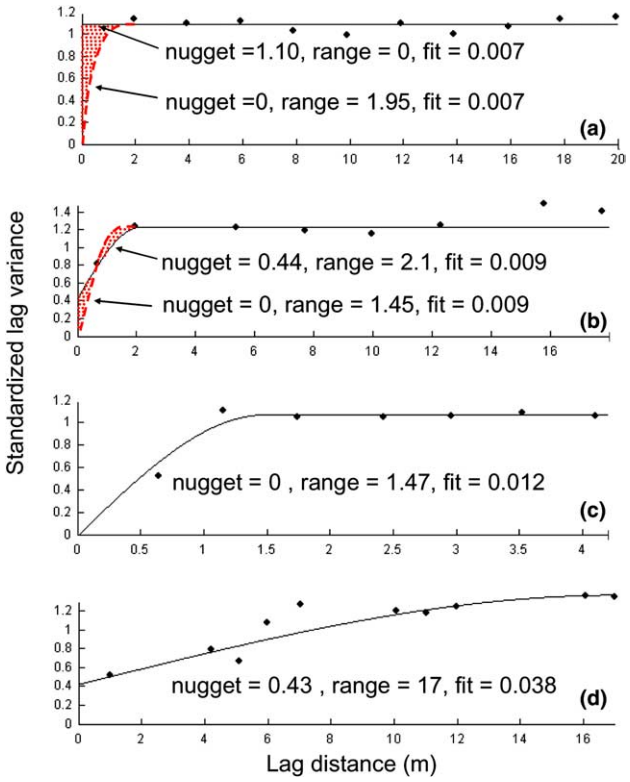

Fig. 1. Examples of four types of standardized variograms encountered when analyzing the spatial patterns of abundance of individual ectomycorrhizal fungal species in the present study: (a) (*Piloderma byssinum*, HJA) a model with no evidence of spatial autocorrelation at the scale studied, leading to an unconstrained nugget and range below the smallest sampling scale, (b) (*Cenococcum geophilum*, PR BPDF) a model in which nugget and range are partially constrained, (c) (*Lactarius fragilis*, SP1) a model with highly constrained nugget and range in which the nugget is zero, (d) (*Lactarius rufus*, PR BP) a model with highly constrained non-zero nugget, and range $\geqslant$ the maximum lag distance. In (a) and (b), solid lines represent the model with the largest nugget; dashed lines represent the models with the smallest nugget. The hatched area is the region of equally-likely models between the two extremes.

Variograms are characterized by variation in the sill, range and nugget. The sill is the background level of variance among samples. The range is the inter-core distance at which the fitted curve reaches the sill, indicating the distance over which spatial autocorrelation (i.e., patchiness in occurrence of species) can be detected. The nugget variance (y intercept of the fitted line) is the variance unexplained by the fitted curve. A large nugget can indicate that much of the spatial autocorrelation in abundance occurred at scales smaller than those sampled, i.e., any patchiness above background levels is at a very small scale. In many cases the nugget variance was large, i.e., unconstrained (e.g., Fig. 1(a)) or only partially constrained (e.g., Fig. 1(b)). In these cases, multiple models ranging from a zero nugget to very large nuggets were possible. In other cases the data were better constrained, leading to a zero or well-constrained non-zero nugget (e.g., Fig. 1(c) and (d)). For this reason, we wished to describe the likely minimum and maximum nuggets and ranges for taxa within those constraints. We calculated a minimum and maximum nugget (y intercept of dashed and solid lines, respectively) and a minimum and maximum range (asymptote of dashed and solid lines, respectively, except that when no range was detected (e.g., solid line, Fig. 1(a)) the minimum range was reported as zero and the asymptote of the dashed line was reported as the maximum range). The distribution of nuggets and ranges was then compared among taxonomic groups for those taxa represented by multiple occurrences. We examined whether minimum and maximum nuggets, and minimum and maximum ranges, differed significantly among taxa, using Kruskal–Wallis tests.

3. Results

3.1. Community level analysis

In all studies community dissimilarity between cores was high at all spatial scales and the relationship between distance and dissimilarity was very noisy (Fig. 2); this reflects the fact that many core samples contained few species in common, and high variation in abundance, independent of their spatial location. Nevertheless, four of the eight sites yielded significant Mantel tests, and seven of the eight showed positive relationships between spatial distance and community distance (Fig. 2). Six of the eight had significant positive spatial autocorrelation using Mantel correlograms, including the four that had significant Mantel tests, plus SP1 and SP2 (Fig. 3). Correlograms using the Sørensen and Steinhaus similarity coefficients gave similar results, so only the former are shown.

The spatial autocorrelation was evident only at a small scale in all but one of the plots of the Mantel test output (Fig. 2). For three of the fours study sites with significant Mantel test results, similarity above background was limited to <3 m (Table 2, Fig. 2(a), (c) and (e)). The study on Bishop pine seedling communities (PR BP seedling) exhibited spatial structure at a slightly smaller scale than any of the studies of mature communities (Table 2). Studies with little or no sampling at <2 m did not exhibit significant spatial structure (Table 2; Fig. 2(b) and (d); Fig. 3), although trends were similar to the other studies. The two studies in which the maximum spatial scale of sampling was less than 7 m also showed no significant spatial pattern in the regular Mantel test (Fig. 2(g) and (h), Table 2), but Mantel correlograms for these sites indicated significant spatial autocorrelation in the smallest distance class (Fig. 3).

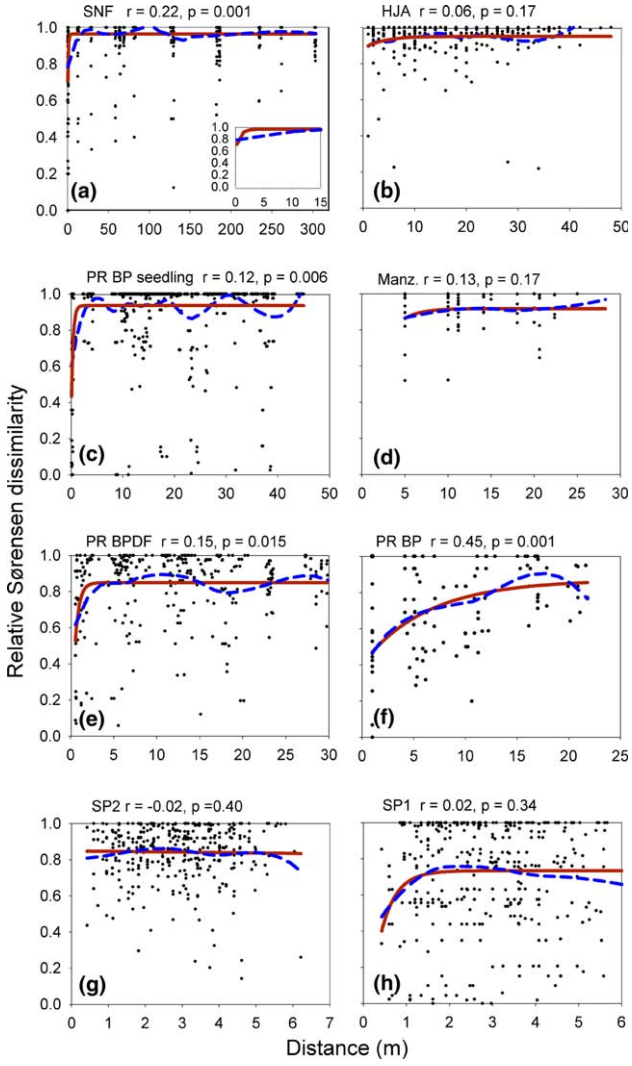

Fig. 2. Plot of output of Mantel tests for spatial structure in ectomycorrhizal fungal communities at several sites, showing pair-wise ectomycorrhizal fungal community Relative Sørensen dissimilarity vs. Euclidean distance for community samples. The r and p value from the Mantel tests are displayed for each graph. To summarize the spatial patterns in the data, we fitted a single, three parameter exponential rise to the maximum (solid line), as well as a smoothed loess fit to the data (dashed line). The maximum value in the exponential rise to the maximum is the "background dissimilarity".

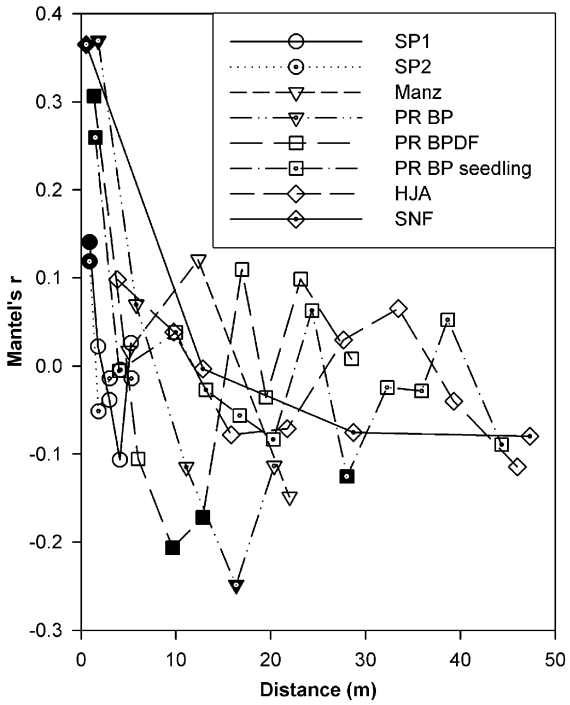

Fig. 3. Mantel correlograms for the ectomycorrhizal fungal communities at eight sites, based on the binary Sørensen similarity coefficient. A significant Mantel's r ($p < 0.05$, Bonferroni corrected) for a distance class is indicated by a filled symbol. Positive correlations in the smaller distance classes indicate positive spatial autocorrelation among community samples. For ease of presentation, the data for SNF are truncated at 45 m. There were no significant correlations beyond this distance. X-axis values for the data points are the mean value of the pair-wise distances within that distance class. Distance class sizes (in m) varied among studies as follows: SP1, 1.20; SP2, 1.20; Manz, 9.4; PR BP, 4.4; PR BPDF, 3.75; PR BP seedling, 3.74; HJA, 6.12; SNF: 10.

The only study in which significant spatial patterns were exhibited at a larger spatial scale was PR BP (Fig. 2(f)). When the exponential rise to the maximum was plotted for the Mantel test data, even at the largest scale (22 m) there was no evidence that background community dissimilarity had been encountered. Extrapolation of the exponential fit to the Mantel test data indicated that 95% of the maximum would be encountered at 15 m, and 99% at 25 m, an order of magnitude higher than the median of all studies (Table 2). In Mantel correlograms, a trend of steadily decreasing spatial autocorrelation with distance, such as seen in the PR BP Mantel test, will result in positive Mantel's r in the smaller distances, and steadily more negative Mantel's r in the larger distances. This is what was clearly seen in the Mantel correlogram for PR BP, a pattern more pronounced than for the other studies (Fig. 3).

The background level of Sørensen dissimilarity varied among studies. There was no significant effect of species richness on the background Sørensen dissimilarity (data not shown). There was, however, a significant rise in background dissimilarity as the sampling scale of the study increased (Fig. 4). This pattern was best described by an exponential rise to the maximum (single, three parameter) if the 300 m scale study was included) or a linear fit if the 300 m scale study was excluded (Fig. 4).

3.2. Individual taxon level analysis

Comparison of relative biomass, relative frequency and variance/mean ratios indicated significant differences among taxonomic groups. The significant difference among groups in relative frequency ($p = 0.01$) was

Table 2
Background Sorensen's dissimilarity (i.e. the maximum value of the Sorensen's dissimilarity index) and distance at which 95% and 99% of background dissimilarity were encountered, when Mantel test output data were fitted with an exponential rise to the maximum at the eight study sites

Site ID	Background Sorensen's dissimilarity	Distance (m) at 95% of background	Distance (m) at 99% of background	Mantel test significant?	Number of pairs <2 m	Max. sampling scale (m)	Number of species
SNF	0.97	1.45	2.60	Y	125	300	50
HJA	0.95	1.35	7.52	N	3	49	42
PR BP seedling	0.94	0.90	1.46	Y	39	45	30
PR BPDF	0.85	1.54	2.31	Y	41	30	16
Manz	0.92	5.30	8.37	N	0	29	40
PR BP	0.87	15.0	25.0	Y	15	22	20
SP1	0.73	1.22	1.80	N	107	6.2	31
SP2	0.85	NA[a]	NA	N	104	6.2	51
Mean	0.89	3.82	7.01				
Median	0.90	1.45	2.60				

Also included are whether the Mantel test was significant, the number of sample pairs that were <2 m apart, the maximum sampling scale and the number of species at each of those sites.

[a] The best fit to the SP2 data did not have a positive slope, so could not be fit with an exponential rise to the maximum.

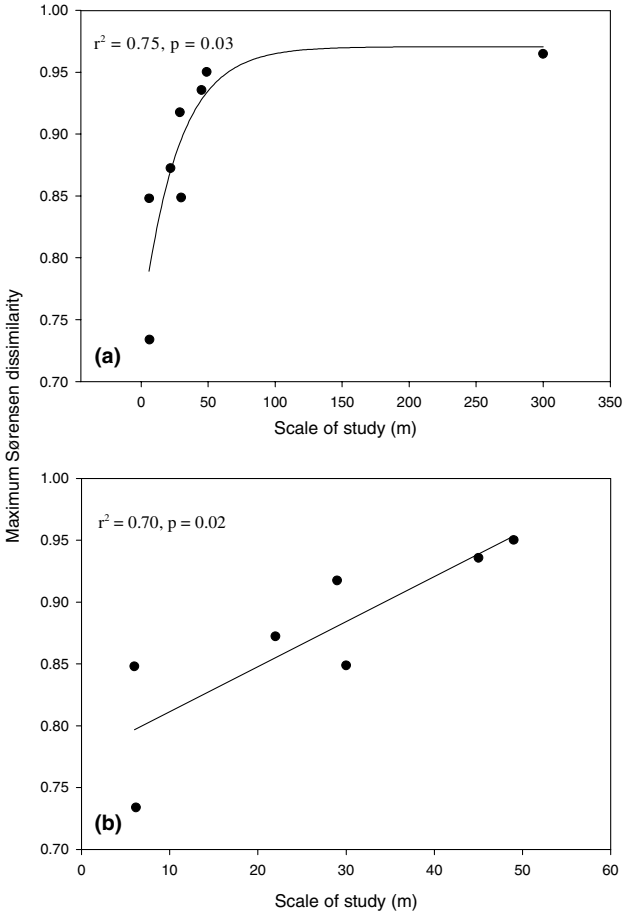

Fig. 4. Maximum Sørensen dissimilarity (background dissimilarity) for ectomycorrhizal fungal communities at different sites as a function of study scale: (a) using the entire dataset, fit with an exponential rise to the maximum, (b) excluding the 300 m scale study site (SNF), with a linear fit.

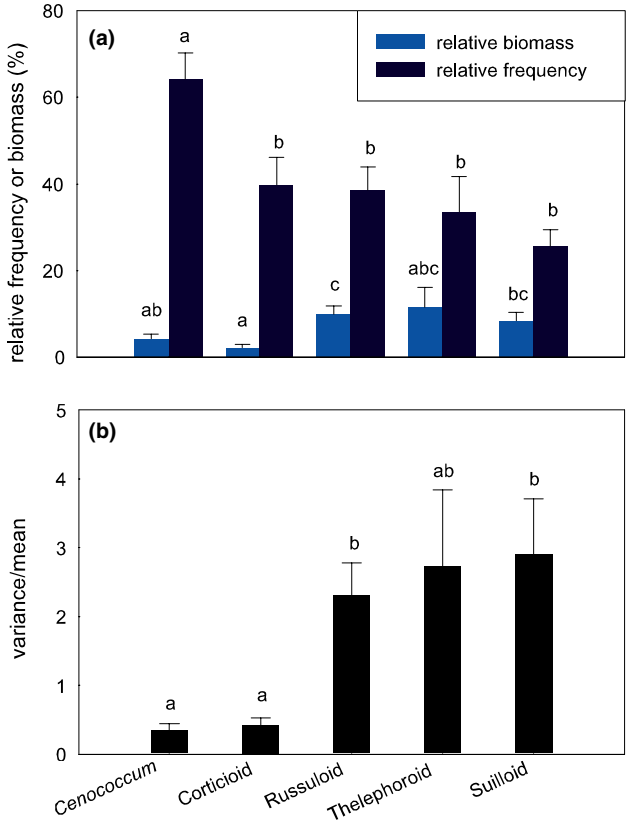

Fig. 5. Comparison of the five ectomycorrhizal fungal taxonomic groups represented by multiple occurrences across sites for (a) mean relative biomass and relative frequency, and (b) variance/mean. Error bars represent standard error. Different letters above columns indicate significant difference, $p < 0.05$. *Cenococcum*, $n = 6$; Corticioid, $n = 5$; Russuloid, $n = 17$; Thelephoroid, $n = 8$; Suilloid, $n = 6$.

driven by the higher frequency of *C. geophilum* than other groups (Fig. 5(a)). There were also significant inter-group differences in relative biomass ($p = 0.01$). *C. geophilum* and the Corticioid group both had lower relative biomass than other groups (Fig. 5(a)). These patterns were reflected in significant inter-group differences in variance/mean (Welch ANOVA, $p = 0.025$). *C. geophilum* and Corticioid species exhibited significantly lower variance/mean ratios than Russuloid and Suilloid taxa (Fig. 5(b)). A similar significant among-taxonomic-group pattern was exhibited when relative abundance/relative frequency was analyzed by group ($p = 0.04$, data not shown). Regression analysis on the whole dataset and on individual taxonomic groups indicated that these patterns were independent of the spatial sampling scale of the study (data not shown).

The standardized variograms agreed in general pattern with the Mantel test results for the entire community. The median minimum and maximum estimated ranges (i.e., the distance below which spatial autocorrelation can be detected) were 1.4 and 2.0, respectively, whereas the corresponding means were 2.19 and 3.44 m, reflecting the left-truncated, right skewed distribution of the data (Fig. 6). The small ranges detected in most taxa were consistent with the results of the Mantel tests of whole community similarity (95% and 99% of background similarity among cores at 1.45 and 2.6 m, respectively). The two species exhibiting the largest scale patterns of spatial autocorrelation ($\geqslant 17$ m, with no sill evident, e.g., Fig. 1(d)) were both Russulaceae spp. at the PR BP site (Appendix A). This site also exhibited the largest scale pattern in the Mantel tests (Fig. 2, Table 2). In many cases, the inter-core distance was not sufficiently small to detect any spatial autocorrelation (e.g., Fig. 1(a)), suggesting that patch size was smaller than the scale sampled, and our maximum range is likely to be an overestimate of patch size. There were no significant differences among taxonomic groups in the minimum and maximum range exhibited (Kruskal–Wallis test, $p = 0.69$ and 0.49, respectively), although the largest maximum ranges were exhibited in the Corticioid (5.31 ± 3.03) and Russuloid (4.34 ± 1.91) groups, and the smallest maximum ranges were in the Suilloid group (2.10 ± 0.76) and *C. geophilum* (2.60 ± 0.58).

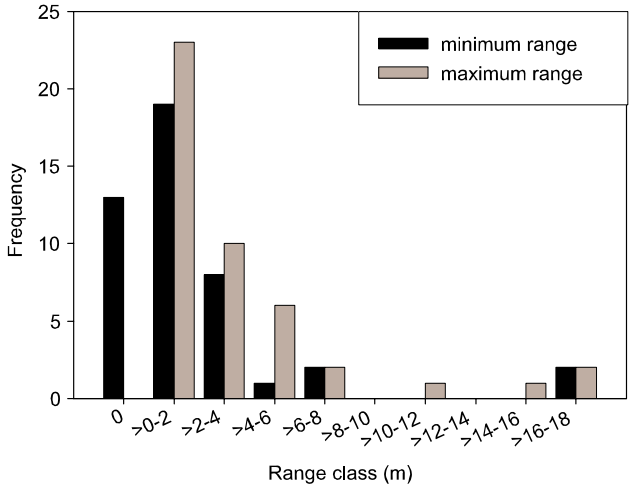

Fig. 6. Histogram of standardized variograms estimates of minimum and maximum ranges for ectomycorrhizal fungal species spatial autocorrelation, pooled for all sites, for the most frequent or abundant taxa.

4. Discussion

4.1. Scale of patchiness

Both community similarity and species-specific patterns suggested that most spatial autocorrelation, or patchiness, detectable by our methods occurred at relatively small spatial scales. These data have implications for design of effective sampling strategies for ectomycorrhizal fungi. Spacing of cores at or beyond the distance where background dissimilarity is encountered should maximize the information gained per core, if the goal of the study is community characterization rather than explicit spatial analysis. This distance was at $\leqslant 2.6$ m in three of the four studies with significant Mantel test results, and 25 m in the fourth. In the Mantel correlograms, only the smallest distance classes exhibited spatial autocorrelation. As data were lumped into classes for this analysis, the exact transition distance is impossible to determine. However, in all but one case these distance classes encompassed the transition distance described by the line fitted to the Mantel test output. The only exception is the PR BP study, where there was no obvious transition to background dissimilarity in the fitted line for the Mantel test output.

The studies with non-significant Mantel test results differed in design from those with significant results, with the former either having few pairs of cores close together, or sampling at a smaller scale. We believe it is likely that the two studies with few or no pairs of cores at <2 m spacing (HJA, Manz) had non-significant Mantel test results because their spacing was larger than in the other studies, i.e., spatial structure was below the scale studied. Two other studies (SP1 and 2) had significant autocorrelation in the Mantel correlograms, but non-significant Mantel tests. These studies had the smallest maximum inter-core distances (<7 m) and also had low background dissimilarities among cores, perhaps because the sampling scale was smaller than patch sizes for the dominant species. When we look at the patterns in the first few meters of the studies with significant Mantel tests, there is little

apparent spatial trend as well. If so, then perhaps sampling at a larger spatial scale would have revealed a stronger spatial trend. Clearly, understanding what factors led to the different patterns among the studies should help guide the development of effective sampling strategies in the future.

Why does one study (PR BP) exhibit stronger spatial pattern than the other seven? This pattern was generated by single large, non-overlapping patches of two dominant species, *Russula brevipe*s and *Lactarius rufus*, and a largely non-overlapping pattern between the former and *Amanita francheti* [13]. *Russula brevipes* was a dominant in two adjacent plots and *L. rufus* was a dominant or sub-dominant in the other three adjacent plots [13]. Variograms showed that these species had the largest patch sizes found in any of the studies.

There are several possible explanations for the observed pattern. First, the study may have been set up over an environmental gradient that generated a spatial trend in mycorrhizal community structure. In fact, the plots were set up over a hill-slope that may have generated a strong gradient. Significant trends in EMF community structure have been found across a much larger scale N deposition gradient [26]. Second, negative associations of fungal species driven by exploitative and interference competition are possible [27,28], although whether this would lead to exclusion zones among certain species pairs is unknown. The presence of multi-species mixtures in individual cores suggests that EMF do not create large-scale monospecific exclusion zones. Indeed, it is common to find multiple species interspersed on neighboring root tips. However, this does not exclude the possibility of negative associations between specific pairs of EMF [29]. Third, the pattern could have been created by the chance sampling of two genets or clusters of individuals. Tests of association are not appropriate in the present study because of the spatial clustering of species occurrences in neighboring cores, and lack of independence among cores [12]. To determine whether this pattern was driven by chance juxtaposition of species patches vs. some pattern of negative association among species would require a much more intensive sampling effort over a larger area, in which multiple independent patches of the species of interest were sampled.

How do the patterns encountered in our analysis compare with others? One other study, using a similar approach to community spatial patterns in *Picea abies* stands [17], found positive spatial correlation in the smallest distance classes analyzed (4–5 and 6–7 m) in sporocarp communities at three sites, as well as in both sporocarps and belowground (molecularly-determined) communities in the smallest distance class measured (4 m) at one site. For their belowground molecular analysis, they did not use cores but rather collected individual root tips at a 1 m spacing interval, identified them, and then pooled them for statistical analysis in 4×4 m blocks. So in pair-wise comparisons of neighboring blocks, the sampling points ranged from 1 to 7.6 m apart. This range encompasses the scale of greater similarity in the present study (<2.6 m). They also analyzed morphotype (= morphologically sorted root tips) communities, although their morphotypes do not strictly represent taxonomically-based communities because of lumping of taxa in some morphotypes. For three of seven subplots they found a similar pattern of positive correlation of morphotype communities over the first 3 m, and negatively correlated in the 6–9 m distance classes. This also agrees quite well with our results.

Other studies have not attempted to look at whole community patterns, but instead have focused on individual recognizable taxa. One study found no evidence for spatial aggregation in *Cenococcum* or *Piloderma* at the 0.1–4.5 m scale, but did find higher similarity among morphotypes in adjacent 1 cm^3 soil volumes [14]. In contrast, two other studies [8,30] found larger-scale patchy distribution of *Piloderma*. In the present study, *Piloderma* exhibited patchiness at a 1.95 m scale, and patches in related Corticioid fungi ranged from 0.74 to 14.1 m (Appendix A). This suggests that there is the potential for formation of larger patches in Corticioid ectomycorrhizal fungi. One study found that mat-forming fungi *Gautieria* and *Hysterangium* formed mycelial patches that were on average <0.5 m diameter and <1 m apart [31], a scale similar to the spatial autocorrelation patterns found for many species in this study.

4.2. Background community dissimilarity

We do not know the cause of the increase in background dissimilarity as sampling scale increased. It is possible that this result is spurious, and that other factors, such as stand composition or age may be driving the pattern. Studies in SNF, HJA and MANZ, with the highest background dissimilarity in the mature stands, were all carried out in mixed-species stands, although in SNF the sampling was focused on ponderosa pine, and in MANZ, Douglas-fir seeds were introduced into a relatively pure *Arctostaphylos glandulosa* stand (with occasional *Quercus wislizenii*). Increasing host diversity might be expected to lead to increasing EMF diversity, which might in turn lead to higher background dissimilarity. However, background dissimilarity was not significantly higher with increasing EMF species richness.

The other study with high background dissimilarity was the PR BP seedling study. The seedlings were in post-fire regeneration sites after stand-replacing fires, and so may have had higher dissimilarity because

genets had only recently developed from point source inoculum (resistant propagules). The degree of dissimilarity in this case would depend on the diversity and distribution of the inoculum sources present in the resistant propagule bank, and their ability to colonize roots rapidly.

It is also possible that sampling a smaller area may affect the background dissimilarity, although the exact mechanism by which that would occur is unclear. It does not appear to be an artifact of doing the calculations with data over different scales: recalculating the equations used to determine background dissimilarity using only the data for the first 13 m for the larger-scaled sites (e.g., SNF, PR BP seedling) did not change the background dissimilarity. One might expect the patterns might be explained by species-area relationships, which would suggest that larger areas would be more species-rich, and higher richness would lead to higher background dissimilarity. However, we found no significant increase in background dissimilarity as species richness increased. Certainly, sampling a larger area would be likely to give a more robust estimate of background dissimilarity, because a larger number of patches and patch boundaries would be encountered, so local variability in estimation of background dissimilarity should be smoothed out. However, this does not explain the greater background dissimilarity.

It is possible that background dissimilarities have not been reached in the smaller-scale studies (SP1, SP2 and PR BP). Indeed, the exponential rise to the maximum for the Mantel test data for PR BP suggests that a larger-scale sampling would have led to higher background dissimilarity at this site.

4.3. Variation in biomass distribution among cores

There were clear interspecific differences in the pattern of biomass distribution among cores. Variance/mean data indicated that certain species exhibited distinct clumps of root tips (e.g., *Rhizopogon*) whereas other taxa exhibited relatively even dispersion of root tips among cores, e.g., *Cenococcum geophilum*. These patterns in variance/mean were not correlated with the minimum or maximum ranges, e.g., *C. geophilum* and Suilloid species exhibited similar minimum and maximum variograms ranges, despite having the most widely divergent variance/mean.

The interspecific differences in variance/mean could arise from a number of different processes. One likely contributing factor is fungal-regulated root proliferation patterns. Suilloid mycorrhizal fungi – *Rhizopogon* and *Suillus* species – commonly stimulate the production of highly clumped coralloid or tuberculate mycorrhizas that contrast with more typical mycorrhizas (Fig. 7b), and may explain why their biomass appears highly clumped in variance/mean analyses. A more detailed analysis of the Suilloid group indicates that the species that form tuberculate root clusters (*Suillus tomentosus, R. vinicolor*) also had the highest variance/mean, whereas species that do not (*R. parksii, R. salebrosus* (reported as *R. subcaerulescens* in our earlier studies), *R. occidentalis* (reported as *R. ochraceorubens* in our earlier studies), *R. ellenae*) had lower variance/mean ratios (Appendix A). *S. tomentosus* and *R. vinicolor* also both had the highest variance/mean for their respective sites (Appendix A). Thus, we must be cautious in combining higher taxonomic groups in an analysis of this sort, because spatial organization is likely to differ significantly even among closely related species. Taxa that consistently exhibited the more even distributions, such as *C. geophilum* and the Corticioid fungi, produce more dispersed branching patterns, and often produce simple, un-branched mycorrhizae.

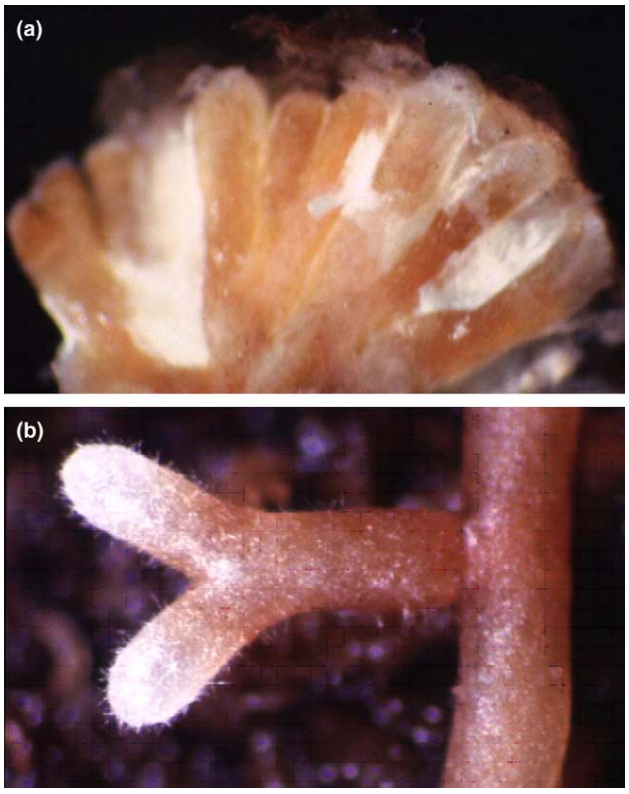

Fig. 7. Mycorrhizas of Bishop pine (*Pinus muricata*): (a) Tuberculate mycorrhiza of *Suillus tomentosus*, split open to reveal clustered individual root tips. (b) Dichotomous mycorrhiza of *Tomentella sublilacina*.

C. geophilum deserves special mention because of the observation of its high frequency despite relatively low biomass across all studies. The observation of high *C. geophilum* frequency is not new [1]. Its high frequency

both within and among studies suggests a remarkably ubiquitous distribution for this fungus. This pattern has not been reported for any other fungus. The ability to detect this pattern may be, in part, due to its morphological distinctness, which makes morphological identification of this species much easier. The causes for its high frequency are unknown, but may arise in part from its formation of vegetative resting structures (sclerotia), which allow it to persist during unfavorable periods [32]. It is also possible that this pattern is at least in part an artifact, because recent phylogenetic analysis suggests that there may be cryptic species in this group [33].

One important implication of taxonomic differences in variance/mean is that species with equal root tip biomass will vary in their probability of being sampled, e.g., the more evenly distributed *C. geophilum* will have a higher probability of being encountered than the patchier *S. tomentosus*, despite the latter's higher mycorrhizal biomass. This will result in a high probability of under-sampling of patchier dominants, especially at low sampling intensity.

4.4. Data limitations

There are some limitations to the data presently available, especially the lack of identification of individuals (i.e., genets) within species. This prevents us from determining whether the spatial patterns discerned represent one or more individuals. Thus we do not know what portions of the observed spatial patterns are driven by patterns of genet size, fragmentation of genets, or aggregations of multiple individuals.

Similar patterns can be interpreted differently in the seedling and mature studies. In the PR BP seedling study large genets were unlikely to have developed in the time since stand-replacing disturbance. The small scale of the patches in this study as indicated by Mantel tests therefore likely indicates the presence of small genets. However, in mature forests, the small patches exhibited might or might not reflect small genets [3]. Suilloid species can often exhibit large genet size [6,7,9,34], but the variograms analysis discerned only relatively small patch sizes in this group (0.63–4.39 m diameter, Appendix A). One of the largest EMF genets recorded ($\geqslant 300$ m^2) was formed by *Suillus pungens* at Point Reyes in Bishop pine forest [6]. However, *Suillus pungens* was only sparsely represented on root tips [6], so would have probably exhibited patchiness at scales smaller than the genet if examined by the present methods.

Furthermore, the converse may also not be true, i.e., large patches may not indicate large genets. Based on sporocarp studies of genet size we can say that not all large aggregations are made up of single genets. For example, the two largest patches in the present study were both formed by Russulaceae, both *Lactarius* and *Russula*. Although genets of *Russula* can sometimes be large [35], not all large patches are necessarily single genets [5]. Genets are not necessarily randomly distributed, but can be clumped, leading to the appearance of multi-individual patches [3]. Thus, other processes, such as positive feedback between high levels of spore rain and establishment rates of genets, or di-mon mating, could lead to patch development, even in the absence of significant vegetative expansion of genets.

In addition, differences in patterns of root anatomy among hosts could affect the species richness and spatial structure of EMF communities. While we have no data to test this hypothesis, the role of host rooting patterns in structuring communities is worth considering in future sampling and analysis.

The next phase in spatial analysis of EMF communities must involve multiple new layers of data collected in studies that were designed explicitly for spatial analyses. First, we must identify individuals of community dominants in both root tips and soil. Next, we must discern how patch structure changes over time. Last, we must link community and population spatio-temporal patterns to factors that could generate such patterns, e.g., endogenous factors such as clonal expansion, high spore rain, di-mon mating, and interspecific interactions; or exogenous factors such as patterns of resource availability, disturbance history and other environmental conditions across a broad range of spatial and temporal scales. These data will help us to unravel the complex processes that generate high diversity and spatial structure in EMF communities, and provide a fuller understanding of the functioning of the mycorrhizal symbiosis in nature.

Acknowledgements

Thanks to Antonio Izzo and Rasmus Kjøller for reading and commenting on a draft of this manuscript. Funding was provided for EAL by NSF research grant DEB 9815262, the Torrey Mesa Research Institute, and the USDA Forest Service, North Central Research Station.

Appendix A

Data on relative biomass, relative frequency, variance/mean and standardized variograms parameters for the more frequent or abundant species at the sites in this study. Species are ordered by taxonomic group. All standardized variograms were fitted with spherical models unless otherwise indicated.

Taxonomic group	ID	Site	Relative biomass (%)	Relative frequency (%)	Variance/ mean	Standardized variogram parameters					
						Indicative goodness of fit	Sill	Min. nugget	Max. nugget	Min. range (m)	Max. range (m)
Amanitaceae	*Amanita francheti*	PR BP	8.9	53.3	1.56	0.05	1.06	0	1.06	0.00	1.00
Amanitaceae	*Amanita pantherina*	PR BP	3.3	33.3	1.59	0.009	1.14	0	0.77	1.80	5.22
Ascomycete	*Cenococcum geophilum*	HJA	5.17	79.2	0.17	0.083	1.16	0	0.37	3.67	4.90
Ascomycete	*Cenococcum geophilum*	Manz	1.27	83.3	0.27	nd[a]	nd	nd	nd	nd	nd
Ascomycete	*Cenococcum geophilum*	PR BPDF	2.8	48.0	0.33	0.009	1.20	0	0.44	1.45	2.10
Ascomycete	*Cenococcum geophilum*	SNF	4.4	52.8	0.24	0.006	1.23	0.61	0.61	2.03	2.03
Ascomycete	*Cenococcum geophilum*	SP1	2.5	55.6	0.21	0.007	1.07	0.41	0.41	2.06	2.06
Ascomycete	*Cenococcum geophilum*	SP2	9.0	66.7	0.84	0.026	1.04	0	0.26	1.61	1.92
Ascomycetes	Helvelloid1	SP2	0.7	33.3	0.12	0.015	1.09	0	1.09	0.00	0.76
Ascomycetes	*Phialophora*-like	PR BP	7.8	26.7	4.58	0.014	1.06	0	1.06	0.00	1.19
Ascomycetes	*Tuber* sp.	PR seedling	19.2	25.6	3.46	0.008	1.17	0	0.43	0.88	4.20
Ascomycetes	*Wilcoxina mikolae*	PR seedling	8.7	17.9	1.91	0.025	1.05	0	0.55	1.13	3.60
Ascomycetes	*Wilcoxina mikolae* 2	PR seedling	5.7	15.4	2.37	nd	nd	nd	nd	nd	nd
Ascomycetes	*Wilcoxina* sp.	PR seedling	8.3	23.1	2.08	0.004	1.08	0.74	0.74	6.46	6.46
Boletoid	*Boletus edulis*	SP1	1.8	22.2	0.60	0.009	1.08	0	0	1.16	1.16
Boletoid	*Xerocomus chrysenteron*	PR BPDF	1.0	16.0	0.32	0.006	1.15	0.57	0.57	6.20	6.20
Coralloid	*Clavulina cristata*	SP1	46.0	74.1	2.01	0.026[b]	1.09	0	0	1.44	1.44
Corticioid	*Amphinema byssoides*	SP2	5.4	63.0	0.47	0.007	1.08	0	1.08	0.00	0.74
Corticioid	*Byssocorticium*-like	HJA	1.11	41.7	0.12	0.017	1.14	0.00	0.94	2.60	14. 10
Corticioid	Corticioid 1	SP1	2.3	29.6	0.82	0.003	1.19	0.77	0.77	4.44	4.44
Corticioid	Corticioid 1	SP2	1.0	18.5	0.26	nd	nd	nd	nd	nd	nd
Corticioid	*Piloderma byssinum*	HJA	1.46	45.8	0.46	0.007	1.10	0	1.10	0.00	1.95
Cortinariaceae	*Cortinarius* 1	SP2	3.5	18.5	1.00	nd	nd	nd	nd	nd	nd
Cortinariaceae	*Cortinarius* 5	SP2	28.1	37.0	8.39	0.012	1.07	0	1.07	0.00	0.65
Cortinariaceae	*Inocybe* 2	SP2	0.4	22.2	0.11	0.003	1.13	0.43	0.43	2.49	2.49

Russuloid	*Lactarius fragilis*	SP1	1.8	25.9	0.52	0.012	1.07	0	0	1.47	1.47
Russuloid	*Lactarius loculentus*	Manz	0.53	33.3	0.20	nd	nd	nd	nd	nd	nd
Russuloid	*Lactarius pseudomucidus*	HJA	3.05	33.3	0.45	0.08	1.10	0	1.10	0.00	3.05
Russuloid	*Lactarius rufus*	PR BP	16.5	46.7	3.34	0.038	1.37	0.43	0.43	17.00	17.00
Russuloid	*Lactarius xanthogalactus*	Manz	15.36	75.0	2.73	nd	nd	nd	nd	nd	nd
Russuloid	*Martellia* sp.	SNF	6.6	13.9	4.35	0.004	1.03	0	1.03	0.00	0.31
Russuloid	*Russula* 1	SP1	0.7	18.5	0.19	nd	nd	nd	nd	nd	nd
Russuloid	*Russula* 1	SP2	10.5	77.8	0.37	0.012	1.09	0	0.6	1.01	1.43
Russuloid	*Russula amoenolens*	PR BPDF	16.0	68.0	1.88	0.014	1.11	0	1.11	0.00	0.80
Russuloid	*Russula brevipes*	PR BP	21.1	40.0	6.67	0.03	1.29	0.84	0.84	17.00	17.00
Russuloid	*Russula placita*	Manz	7.3	16.7	3.31	nd	nd	nd	nd	nd	nd
Russuloid	*Russula* sp.	HJA	4.81	16.7	2.33	nd	nd	nd	nd	nd	nd
Russuloid	*Russula xerampelina*	PR BPDF	10.0	36.0	2.96	0.002	1.16	0	0.51	1.22	2.23
Russuloid	Russuloid 1	Manz	10.66	41.7	2.91	nd	nd	nd	nd	nd	nd
Russuloid	Russuloid 1	PR seedling	1.6	25.6	0.48	0.045	1.05	0	1.05	0.00	0.20
Russuloid	Russuloid 1	SNF	23.0	16.7	4.69	0.02	1.41	0.28	0.28	3.32	3.32
Russuloid	Russuloid 1	SP2	7.6	33.3	2.00	0.009	1.05	0	1.05	0.00	0.96
Russuloid	Russuloid 32	Manz	11.1	8.3	11.06	nd	nd	nd	nd	nd	nd
Suilloid	*Rhizopogon ellenae*	SP1	8.4	18.5	3.72	0.012	1.03	0	1.03	0.00	0.63
Suilloid	*Rhizopogon occidentalis*	PR seedling	9.3	20.5	2.87	0.005	1.10	0	0.96	0.37	4.39
Suilloid	*Rhizopogon parksii*	Manz	0.61	25.0	0.19	nd	nd	nd	nd	nd	nd
Suilloid	*Rhizopogon parksii*	PR BPDF	6.4	44.0	1.05	0.046	1.18	0.12	0.12	1.51	1.51
Suilloid	*Rhizopogon salebrosus*	SNF	9.4	19.4	3.89	0.014	1.08	0.99	0.99	3.32	3.32
Suilloid	*Rhizopogon vinicolor*	HJA	11.67	8.3	9.74	nd	nd	nd	nd	nd	nd
Suilloid	*Suillus tomentosus*	SP1	15.9	25.9	5.65	0.004	1.05	0	1.05	0.00	0.63
Thelephoroid	Thelephoroid 1	SP2	1.0	18.5	0.31	nd	nd	nd	Nd	nd	nd
Thelephoroid	Thelephoroid 13	HJA	12.72	16.7	6.11	nd	nd	nd	Nd	nd	nd
Thelephoroid	Thelephoroid 2	PR BPDF	15.0	44.0	2.57	0.024	1.13	0	0	3.15	3.15
Thelephoroid	Thelephoroid 2	SNF	1.5	16.7	0.62	0.004	1.10	0	0.94	0.80	10.80
Thelephoroid	*Tomentella* 2	SP2	1.0	22.2	0.33	0.001	1.09	0	0	1.60	1.60
Thelephoroid	*Tomentella* 4	SP2	0.7	18.5	0.24	nd	nd	nd	Nd	nd	nd
Thelephoroid	*Tomentella sublilacina*	PR BP	30.4	80.0	2.84	0.023	1.18	0	1.18	1.40	5.30
Thelephoroid	*Tomentella sublilacina*	PR BPDF	30.2	52.0	8.77	0.025	1.11	0	0.8	1.01	2.00

[a] No variograms were generated for the Manz site because of the low number of cores, or for species with low frequency at other sites.
[b] Gaussian mode.

References

[1] Horton, T.R. and Bruns, T.D. (2001) The molecular revolution in ectomycorrhizal ecology: peeking into the black-box. Mol. Ecol. 10, 1855–1871.

[2] Bruns, T.D. (1995) Thoughts on the processes that maintain local species-diversity of ectomycorrhizal fungi. Plant Soil 170, 63–73.

[3] Taylor, A.F.S. (2002) Fungal diversity in ectomycorrhizal communities: sampling effort and species detection. Plant Soil 244, 19–28.

[4] Agerer, R. (2001) Exploration types of ectomycorrhizae – a proposal to classify ectomycorrhizal mycelial systems according to their patterns of differentiation and putative ecological importance. Mycorrhiza 11, 107–114.

[5] Redecker, D., Szaro, T.M., Bowman, R.J. and Bruns, T.D. (2001) Small genets of *Lactarius xanthogalactus, Russula cremoricolor* and *Amanita francheti* in late-stage ectomycorrhizal successions. Mol. Ecol. 10, 1025–1034.

[6] Bonello, P., Bruns, T.D. and Gardes, M. (1998) Genetic structure of a natural population of the ectomycorrhizal fungus *Suillus pungens*. New Phytol. 138, 533–542.

[7] Dahlberg, A. and Stenlid, J. (1994) Size, distribution and biomass of genets in populations of *Suillus-bovinus* (L, Fr) Roussel revealed by somatic incompatibility. New Phytol. 128, 225–234.

[8] Dahlberg, A. (1997) Population ecology of *Suillus variegatus* in old Swedish Scots pine forests. Mycol. Res. 101, 47–54.

[9] Zhou, Z.H., Miwa, M. and Hogetsu, T. (2000) Genet distribution of ectomycorrhizal fungus *Suillus grevillei* populations in two *Larix kaempferi* stands over two years. J. Plant Res. 113, 365–374.

[10] Fiore-Donno, A.M. and Martin, F. (2001) Populations of ectomycorrhizal *Laccaria amethystina* and *Xerocomus* spp. show contrasting colonization patterns in a mixed forest. New Phytol. 152, 533–542.

[11] Gryta, H., Debaud, J.C. and Marmiesse, R. (2000) Population dynamics of the symbiotic mushroom *Hebeloma cylindrosporum*: mycelial persistence and inbreeding. Heredity 84, 294–302.

[12] Dale, M.R.T. (1999) Spatial Pattern Analysis in Plant Ecology. Cambridge University Press, Cambridge, UK. 326 pp.

[13] Taylor, D.L. and Bruns, T.D. (1999) Community structure of ectomycorrhizal fungi in a *Pinus muricata* forest: minimal overlap between the mature forest and resistant propagule communities. Mol. Ecol. 8, 1837–1850.

[14] Jonsson, L., Dahlberg, A. and Brandrud, T.-E. (2000) Spatiotemporal distribution of an ectomycorrhizal community in an oligotrophic Swedish *Picea abies* forest subjected to experimental nitrogen addition: above- and below-ground views. Forest Ecol. Manage. 132, 143–156.

[15] Grogan, P., Baar, J. and Bruns, T.D. (2000) Below-ground ectomycorrhizal community structure in a recently burned bishop pine forest. J. Ecol. 88, 1051–1062.

[16] Mantel, N. (1967) The detection of disease clustering and a generalized regression approach. Cancer Res. 27, 209–220.

[17] Peter, M., Ayer, F., Egli, S. and Honegger, R. (2001) Above- and below-ground community structure of ectomycorrhizal fungi in three Norway spruce (*Picea abies*) stands in Switzerland. Can. J. Bot. 79, 1134–1151.

[18] Klironomos, J.N., Rillig, M.C. and Allen, M.F. (1999) Designing belowground field experiments with the help of semi-variance and power analyses. Appl. Soil Ecol. 12, 227–238.

[19] Horton, T.R., Bruns, T.D. and Parker, V.T. (1999) Ectomycorrhizal fungi associated with *Arctostaphylos* contribute to *Pseudotsuga menziesii* establishment. Can. J. Bot. 77, 93–102.

[20] McCune, B. and Mefford, M.J. (1999) PC-ORD. Multivariate Analysis of Ecological Data. MJM Software Design. Gleneden Beach, Oregon, USA.

[21] Casgrain, P. and Legendre, P. (2004). The R Package for Multivariate and Spatial Analysis, Version 4.0 (Development Release 7). Department of Biological Sciences, University of Montreal, Montreal, Canada.

[22] Ripley, B.D. (1981) Spatial statistics. John Wiley & Sons, New York, USA.

[23] SAS Institute. (1989–1999) JMP. SAS Institute, Inc., Cary, NC.

[24] Pannatier, Y. (1993–1996) Variowin: Software for Spatial Data Analysis in 2D (Software). Springer-Verlag, New York, USA.

[25] Pannatier, Y. (1996) Variowin: Software for Spatial Data Analysis in 2D (User's manual). Springer-Verlag, New York, USA.

[26] Lilleskov, E.A., Fahey, T.J., Horton, T.R. and Lovett, G.M. (2002) Belowground ectomycorrhizal fungal community change over a nitrogen deposition gradient in Alaska. Ecology 83, 104–115.

[27] Lockwood, J.L. (1992) Exploitation competition. In: The fungal community: its organization and role in the ecosystem, 2nd Edn. (Carroll, G.C. and Wicklow, D.T., Eds.), pp. 243–263. Marcel Dekker, New York, USA.

[28] Wicklow, D.T. (1992) Interference competition. In: The fungal community: its organization and role in the ecosystem, 2nd Edn. (Carroll, G.C. and Wicklow, D.T., Eds.), pp. 265–274. Marcel Dekker, New York, USA.

[29] Agerer, R., Grote, R. and Raidl, S. (2002) The new method 'micromapping', a means to study species-specific associations and exclusions of ectomycorrhizae. Mycological Progress 1, 155–166.

[30] Danielson, R.M. and Visser, S. (1989) Effects of forest soil acidification on ectomycorrhizal and vesicular arbuscular mycorrhizal development. New Phytol. 112, 41–47.

[31] Griffiths, R.P., Bradshaw, G.A., Marks, B. and Lienkaemper, G.W. (1996) Spatial distribution of ectomycorrhizal mats in coniferous forests of the Pacific Northwest, USA. Plant Soil 180, 147–158.

[32] Miller, S.L., Torres, P. and Mcclean, T.M. (1994) Persistence of basidiospores and sclerotia of ectomycorrhizal fungi and *Morchella* in soil. Mycologia 86, 89–95.

[33] Douhan, G. and Rizzo, D. (2003) Fine scale genetic structure analysis of *Cenococcum geophilum* reveals putative cryptic species. In: Annual Meeting of the Mycological Society of America, vol. 54, Pacific Grove, CA, USA, pp. 18–19.

[34] Dahlberg, A., Jonsson, L. and Nylund, J.E. (1997) Species diversity and distribution of biomass above and below ground among ectomycorrhizal fungi in an old-growth Norway spruce forest in south Sweden. Can. J. Bot. 75, 1323–1335.

[35] Bergemann, S.E. and Miller, S.L. (2002) Size, distribution, and persistence of genets in local populations of the late-stage ectomycorrhizal basidiomycete, *Russula brevipes*. New Phytol. 156, 313–320.

[36] Stendell, E.R., Horton, T.R. and Bruns, T.D. (1999) Early effects of prescribed fire on the structure of the ectomycorrhizal fungus community in a Sierra Nevada ponderosa pine forest. Mycol. Res. 103, 1353–1359.

[37] Horton, T.R. and Bruns, T.D. (1998) Multiple-host fungi are the most frequent and abundant ectomycorrhizal types in a mixed stand of Douglas fir (*Pseudotsuga menziesii*) and bishop pine (*Pinus muricata*). New Phytol. 139, 331–339.